



INTRA AND INTERMOLECULAR HYDROGEN BONDING IN POLYSACCHARIDE REINFORCEMENTS: THEIR EFFECTS ON THE MECHANICAL PROPERTIES OF POLYLACTIDE

AUTHORS:

O. P. Gbenedor^{1,2*} and A. P. I. Popoola²

AFFILIATIONS:

¹ Department of Metallurgical and Materials Engineering, University of Lagos, Lagos, NIGERIA

²Department of Chemical, Metallurgical and Materials Engineering, Tshwane University of Technology, Pretoria, SOUTH AFRICA

*CORRESPONDING AUTHOR:

Email: ogbenedor@unilag.edu.ng

ARTICLE HISTORY:

Received: December 28, 2024.

Revised: August 28, 2025.

Accepted: September 11, 2025.

Published: January 03, 2026.

KEYWORDS:

Biocomposite, Cellulose, Cornstalk FTIR, Hydrogen bond, Lignin, Polylactide.

ARTICLE INCLUDES:

Peer review

DATA AVAILABILITY:

On request from author(s)

EDITORS:

Chidozie Charles Nnaji

Abstract

FUNDING:

None

In this work, cellulose (CSC) and lignin (CSL), chemically sourced from cornstalk (CS), were separately used as reinforcement on polylactide (PLA). The aim was to evaluate the influence of intra and intermolecular hydrogen bond interactions in these polysaccharides on the mechanical properties of PLA. Cellulose was synthesized from 100 μm CS particles using 1 M NaOH, while 1 M HCl was used in extracting (CSL) from CS. Biocomposite containing 20 wt. % of each reinforcement was cast into tensile and flexural test specimens. The average hydrogen bonding E_H calculated from Fourier Transform Infrared spectroscopy (FTIR) within the OH region of CSC was 4.63 kCal, while that from synthesized CSL was 4.47 kCal. Furthermore, the average bond distance R (evaluated from FTIR) was 2.78 and 2.83 \AA for CSC and CSL, respectively. Both reinforcements improved the tensile properties of PLA, but the composite (PLA/CSC) with CSC as reinforcement gave a better result. The tensile strength increased from 30.1 MPa in PLA to 45.5 and 67 MPa in PLA/CSL and PLA/CSC, respectively. Unreinforced PLA began to yield from 15.1 MPa, while PLA/CSL and PLA/CSC commenced yielding from 39.4 and 54.8 MPa, respectively. The maximum elastic modulus (2.32 GPa) was maintained by PLA/CSC, while unreinforced PLA possessed a modulus of 1.96 GPa. The poorest response to elongation under tension (0.9 %) was recorded by unreinforced PLA, and PLA/CSC reached 4.7 % of its initial length before fracture. The addition of CSC to PLA raised the flexural modulus and strength of PLA by 61.2 and 187.8 %, respectively. Morphology of the PLA fractured surface, analyzed via Scanning Electron Microscope (SEM), revealed minor cracks with flakes; the fractured surface was not as rough as that of PLA/CSC and PLA/CSL. This showed that unreinforced cast PLA displayed a brittle-like feature.

HOW TO CITE:

Gbenedor, O. P. and Popoola, A. P. I. "Intra and Intermolecular Hydrogen Bonding in Polysaccharide Reinforcements: their Effects on The Mechanical Properties of Polylactide", *Nigerian Journal of Technology*, 2025, 44(4), pp. 557 - 566. <https://doi.org/10.4314/njt.2025.4570>

1.0 INTRODUCTION

There has been a profound and recurring clamour for the use of renewable materials for science and engineering applications in recent years because they are environmentally friendly and cheap to synthesize. Among the existing classes of materials, biopolymers are not only eco-friendly – they are also biocompatible with living tissues [1]. Their lightweight and multiple functionalities have made them useful in all spheres of science and technology, especially in recent times when every society now decries the negative influences of fossil fuel usage [2-3].

Among the biopolymers are starch, chitin, chitosan, cellulose, lignin, gelatin, and protein [4-10]. An additional feature these polymers possess aside from their biocompatibility and versatility is their biodegradability; this offers them a big advantage over synthetic polymers such as polyethylene, Teflon, and epoxy. In tissue engineering, a widely used and often investigated biopolymer is polylactide (PLA); it is a linear aliphatic polyester that has been wholly sourced from corn and potato starch [11-12]. Processing of PLA has been carried out by film casting [13], extrusion [14], injection moulding [15], fiber spinning [16], and additive manufacturing [15]. These processing techniques are enabled due to their greater ease of thermal processing than other biomaterials. Polylactide has faced some drawbacks because of its brittleness and poor flexibility [17]. A conventional way to improve the mechanical strength of PLA is by forming a composite with other bio-based lignocellulosic fillers such as cellulose and lignin; both are polysaccharides. A major component that imparts mechanical strength to every plant cell wall is cellulose, which is the most abundant biopolymer on earth. Lignin, on the other hand, is a cross-linked biopolymer that provides stiffness and mechanical strength to plant cell walls. It is necessary for the support of the plant's internal components.

The mechanical strength of cellulose is derived from its hydrogen bond structure and chemical modifications (done to alter its structure for other desired features). Wang et al. [18] reported that the tensile strength of cellulose sheets synthesized from water bamboo reduced from 18.34 MPa to 10.89 MPa. The reduction in strength was attributed to the alteration of its hydrogen bond structure engendered by surface modification with a silane coupling agent. According to the researchers, the aim of this agent was to improve interfacial compatibility between PLA and cellulose. In an earlier study [19], it was reported that the hydrogen bond in cellulose can be influenced by the synthesis method employed. The amount (wt. %) of cellulose in the PLA matrix is also a contributing factor to PLA/cellulose mechanical properties. When 0.25 % softwood pulp cellulose nanofibril was added to PLA, Zhang et al. [20] noticed that the increase in the composite's (3D printed nanofiber) tensile strength and elastic

modulus was minimal; increasing the content to 0.5 % yielded a more conspicuous increase, and the most profound results were achieved using 1 % cellulose. In addition to this, they stressed that increasing cellulose content in the PLA matrix will foster good interfacial bonding between the matrix and reinforcement.

This further supports the investigations of Agbakoba et al. [21] and Bononad et al. [22], who affirmed that cellulose provides a good reinforcing effect on PLA. Previous studies have shown that lignin serves as a good reinforcement for PLA; the tensile strength of electrospun PLA fiber (0.19 MPa) was increased to 0.3 and 1.19 MPa after adding corn chaff and coconut husk-sourced lignin, respectively [23]. Most of the time (depending on source and isolation method), compatibilizers are added to PLA/lignin composites to support effective interfacial bonding, with lignin playing a major role in the strengthening effect [24-28]. Although it has been established that OH functional groups in cellulose with phenolic and aliphatic OH groups in lignin are responsible for the strengths of these polysaccharides, the effects of the magnitudes of their intra and intermolecular hydrogen bond features (within their respective OH groups) on the mechanical properties of PLA need to be investigated. In this study, cellulose and lignin are synthesized from cornstalk (CS) and used as reinforcement on PLA. Corn straw (corn stover) in farming is the most generated waste in comparison with other grain crops [29], consisting of stalk, cob, leaves, and husk. Cornstalk makes up 50 % of the total corn plant and has been a useful source of biogas and oil [30]. The hydrogen bond features in CS cellulose and lignin were evaluated and their influence as reinforcement materials on the mechanical properties of PLA is studied.

2.0 METHODOLOGY

2.1 Cellulose and Lignin Extraction from CS with Composites Preparation

Cornstalks were dried and pulverized into 100 μ m particle sizes. To eliminate lignin and hemicellulose from CS, the particles were soaked in 1 M NaOH and continuously stirred for 2 h. The solution was filtered as both lignin and hemicellulose were dissolved into the filtrate while the residue contained cellulose; this was washed with distilled water to neutral pH and oven dried at 50 °C to complete dryness. To isolate lignin from CS, 30 % v/v of diethyl ether was mixed with the particles and allowed to soak for 24 h to remove possible extractives that may be contained in



the biomass. At the end of this period, the residue was washed with distilled water, filtered, and dried at 50 °C in an oven. Cellulose and hemicellulose were isolated by reacting the particles with 10 M HCl at 100 °C for 3 h. The residue (lignin) was washed and dried as previously done. In this study, cellulose and lignin isolated from CS are designated CSC and CSL, respectively. Each reinforcement (20 wt. %) was charged into molten PLA (MW 250,000 g/mol) at 170 °C in the heating chamber of a compounding machine. The device was designed with a stirrer (attached to an electric motor), which completely stirred the mixture to achieve a thorough distribution of reinforcement in the matrix. The mixture was cast into dog-bone-shaped specimens (in a steel mould) for tensile tests following ASTM D638 standards. Melts were also cast into flexural test specimens in accordance with ASTM D790 standards.

2.2 Characterizations

2.2.1 Fourier transform infrared spectroscopy (FTIR)

To decipher the functional groups present in the structures of isolated CSC and CSL, a UATR Two spectrometer was used. At different times, 10 mg of CSL and CSC particles were dispersed in KBr. Employing a scan rate of 4 cm⁻¹, absorbance measurements were taken between wavenumbers 4000 and 500 cm⁻¹.

2.2.2 Tensile test

The stiffness, tensile strength (UTS), elongation at break, yield, and fracture stress of each prepared tensile specimen (PLA, PLA/CSC, and PLA/CSL) were tested using an Instron tensile testing machine. At room temperature, each sample, which was firmly held at both ends by the gauge of the equipment, was subjected to an applied tensile load at 10 mm/min. The values of the instantaneous loads with their corresponding displacements were recorded, and stress-strain curves were plotted.

2.2.3 Flexural test

Three-point flexural testing was conducted using a Testometric Universal Testing Machine in accordance with ASTM D790 standard. A cross-head speed of 30mm/min, maintained at a span of 100mm, was employed for each sample. Flexural strength and modulus were measured from this technique.

2.2.4 Scanning electron microscopy (SEM)

Morphological features of PLA, PLA/CSC, and PLA/CSL were investigated using a VEGA 3 TESCAN scanning electron microscope.

3.0 RESULTS AND DISCUSSION

3.1 Functional Groups and OH Bonding in Extracted Polysaccharides

The spectra shown in Figure 1a demonstrate the active functional groups present in CS, CSC, and CSL. The spectrum of CS is comparable to that reported for other lignocellulosic biomass such as bamboo, albezia pods, brewery spent grain, and corn chaff [19], [23], [31-32]. This could be a result of the fact that all plant biomass contains some similar organic constituents/compounds (they may vary in amounts). To justify the efficacy of the two polysaccharides' isolation from CS, Table 1 shows the functional groups present in CSC and CSL. Both spectra look similar, but there exist some functional groups that are peculiar to either polysaccharide. As mentioned for CS, the spectra results of CSC and CSL are similar to cellulose and lignin synthesized from other biomass [23], [33-34]. This could be attributed to the fact that they are lignocellulose in nature. Within the OH stretching of CSC (between 3600 and 3000 cm⁻¹), it has been reported that there exist an intermolecular ((3)H...O(5)) and two intramolecular (O(2)H...O(6) and O(3)H...O(5)) hydrogen bonds. As adopted by Ciolacu et al. [35], the hydrogen bond energy E_H (kCal) in CSC was determined using Equation (1). This equation has also been used in calculating hydrogen bond energy for biomass-sourced polysaccharides in earlier studies [19], [36-37].

$$E_H = [1/k \times (V_o - V)/V_d] \quad (1)$$

Frequency attributed to free OH groups at 3600 cm⁻¹ is represented by V_o. V is the frequency of the bonded OH groups and k = 1.68 x 10⁻² kcal⁻¹. The bond distance R in each bond was determined using Equation (2)

$$\Delta V = 4430 (2.84 - R) \quad (2)$$

The wavenumber of each bond was determined by deconvolution between 3600 and 3000 cm⁻¹ using the Gaussian method (R² = 0.99). At 3412 and 3293 cm⁻¹, there exist O(2)H...O(6) and O(3)H...O(5) respectively for CSC intramolecular hydrogen bonds (Figure 1b); O(6)H...O(3) intermolecular bond is absorbed on 3256 cm⁻¹. This bond maintains the highest occupancy (68.46 %) in CSC (Figure 1b and

Vol. 44, No. 4, December, 2025



© 2025 by the author(s). Licensee NIJOTECH.

This article is open access under the CC BY-NC-ND license.

<https://doi.org/10.4314/njt.2025.4570>

<http://creativecommons.org/licenses/by-nc-nd/4.0/>

Table 2). The magnitudes of E_H possessed by each bond are displayed in Table 2. The average E_H and R for CSC are calculated to be 4.63 kCal and 2.78 Å.

In CSL, within the OH region, free OH groups (in alcoholic compounds) occur within (3616 – 3640 cm^{-1}); intra and intermolecular hydrogen bonds exist on 3550 – 3560 cm^{-1} and 3520 – 3480 cm^{-1} , respectively [38]. These bands were identified by plotting a second derivative of CSL spectra within the OH region [32], [39] as shown in Figure 2. Results from this study show that the intramolecular hydrogen bond (in phenolic groups) is formed on 3554 and 3577 cm^{-1} , while the intermolecular hydrogen bond is found on 3528 cm^{-1} . Wavenumber shifts ($\Delta\nu_{\text{OH}}$)

within hydrogen-bonded structures were used in determining the average strength of both inter and intramolecular interactions in CSL (Table 3). The magnitudes of $\Delta\nu_{\text{OH}}$ were used in determining the hydrogen bond enthalpy (ΔH) of CSL (equivalent to its hydrogen bond energy) using Equation (3) [40].

$$-\Delta H (\text{kCal/mol}) = 0.016 \Delta\nu_{\text{OH}} + 0.63 \quad (3)$$

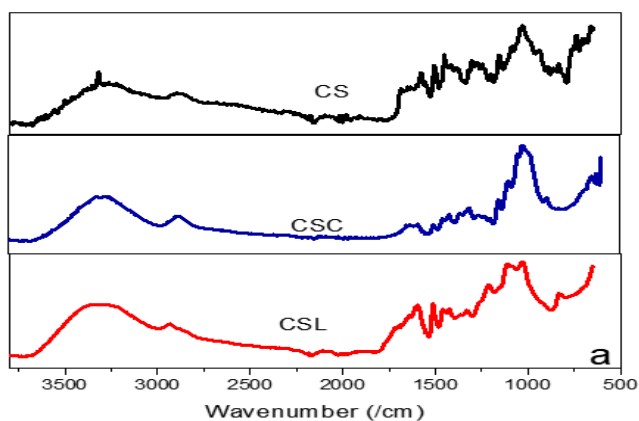


Table 1: Functional groups of CS, CSC and CSL

Functional groups	CS	CSC	CSL
OH vibrations	3286	3331, 3295	3343, 3313
CH stretching	2882	2866	2908
C=C in benzene ring	1529	--	1587
C=O and CH (carbonyl and caboxylate)	1452	1406	1466
OH vibration (Syringyl ring)	--	--	1212
CO-C stretching	1153	--	--
C-O (alcohol and phenols)	1074	--	1092
C-O and C-C (glycosydic linkage)	1020	1026	--

Cellulose and hemicellulose

C-H deformations	929	892	--
------------------	-----	-----	----

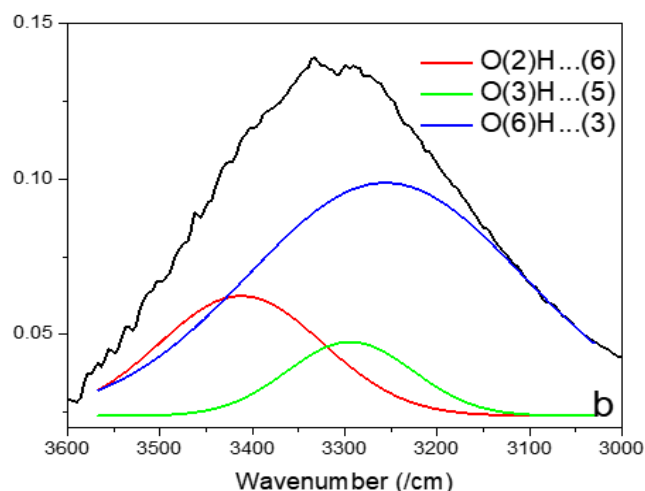


Figure 1: (a) FTIR spectra of CS, SC and CSL (b) FTIR spectra of CSC spectrum showing the intra and intermolecular hydrogen bonds between 3600-3000 cm^{-1} .

Table 2: Band assignment to the OH band (3600-3000 cm^{-1}) in CSC with their E_H and R values

Wave number (cm^{-1})	Amount (%)	E_H (kCal)	R (Å)
O(2)...(6)	21.05	3.11	2.80
O(3)...(5)	10.49	5.08	2.77
O(6)...(3)	68.46	5.69	2.76

Table 3: Wavenumber shifts of CSL from the second derivative of the FTIR spectrum, their bond enthalpies, and R values

Sample wavenumber (cm^{-1})	$\Delta\nu_{\text{OH}}$ (cm^{-1})	$-\Delta H$ (kCal/mol)	$-R$ (Å)
3577	264	4.85	2.83
3554	241	4.49	2.83
3528	215	4.07	2.82



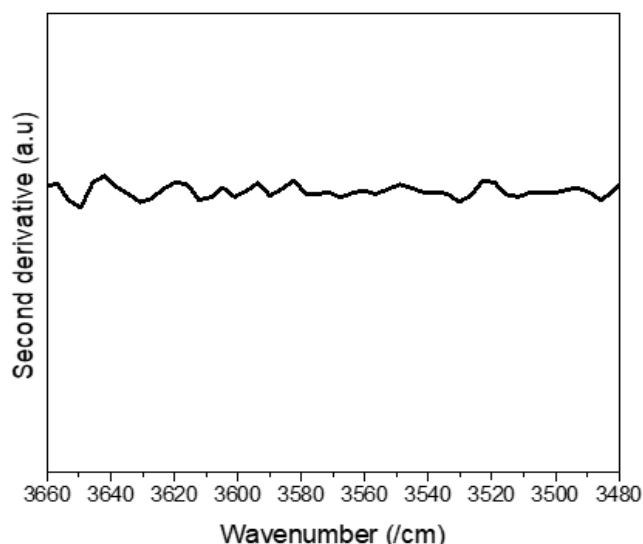


Figure 2: FTIR (second derivative) spectrum of CSL

3.2 Mechanical Properties of PLA, PLA/CSC and PLA/CSL

Figure 3 shows the tensile properties of PLA, PLA/CSC, and PLA/CSL. The tensile strength, which is the maximum stress, achieved by each material before fracture (UTS), increases from 30.1 MPa (for PLA) to 45.5 and 67 MPa in PLA/CSL and PLA/CSC, respectively. The increase in the UTS for the composites can be attributed to the possibility of a strong interaction between PLA and each reinforcement. It has been reported that functional groups containing OH and CH₃, which are present in PLA molecules, enhance interfacial interactions (with reinforcements), which eventually improve mechanical properties such as shear strength and fracture toughness of its composites [41]. Xia et al. [42] and Zhao et al.

[43] affirmed that cellulose and lignin also possess these functional groups (also confirmed in this study); this may be the reason for the improvement in UTS observed in the composites, knowing that CSC and CSL contain these interfacial adhesion-enhancing functional groups. In some polymer composites, agglomeration of reinforcement can engender improper matrix/reinforcement interfacial bonding. A scenario such as this was reported in the investigation of Gorgun et al., [44], where PLA was reinforced with 2, 3 and 5 wt. % microcrystalline cellulose particles. Reduction in the tensile strengths of composites compared to that of unreinforced PLA was ascribed to a poor transmission of stress across the PLA/reinforcement interface caused by agglomerations of microcrystalline reinforcement. This, according to the researchers, contributed to poor interfacial bonding. In this study, PLA begins to

yield (yield stress, indicated by an arrow) from 15.1 MPa, while PLA/CSL and PLA/CSC commence yielding from 39.4 and 54.8 MPa, respectively, under tension. The tensile stress-strain relationship indicates that PLA/CSC possesses the maximum elastic modulus (2.32 GPa), followed by PLA/CSL (2.02 GPa), and the least by PLA (1.96 GPa). Fracture strength and elongation at break of PLA are improved by adding CSC and CSL (Figure 3); PLA/CSC fractures at 56.9 MPa, while PLA/CSL and PLA fracture after 41.3 and 23.4 MPa, respectively, are attained. Polylactide has the poorest elongation under tension (0.9 %); the highest is recorded for PLA/CSC, where it stretches up to 4.7 % of its original length before fracture. The addition of CSL also contributes to the improvement of PLA elongation in response to tensile load, as it expands longitudinally by 3.9 % before complete failure. Johansson et al. [45] reported that the addition of acetylated lignin to PLA elevated its elongation at break and impact strength as a result of reduced reinforcement agglomeration that occurred. However, its UTS and elastic modulus were lower than that of unreinforced PLA. Although the reason(s) for this were not mentioned, the high concentration of C=O present in the CSL (as a result of chemical modification) may be responsible for this. Makri et al. [46] alluded lignin's contribution to PLA's improved tensile strength and elastic modulus to its rigidity, which was brought about by the concentration of benzene rings in its structure; in addition to this, the researchers added that stereocomplexion in lignin's structure gave room for an easy transfer of load from PLA and this further encourages dispersion of lignin in PLA.

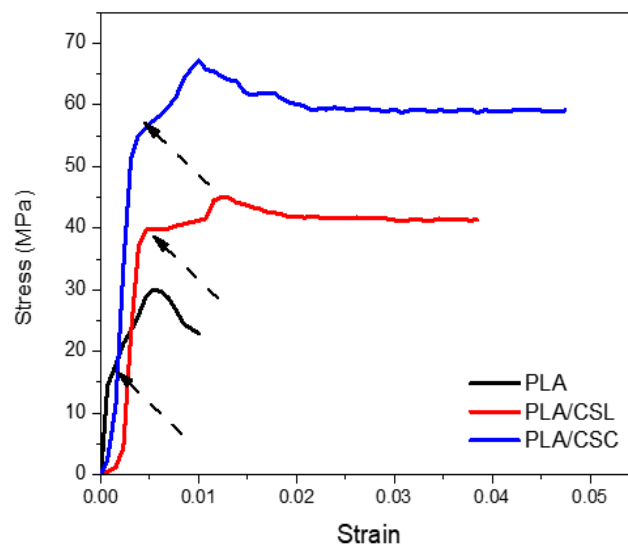


Figure 3: Stress-strain curves for PLA, PLA/CSC, and PLA/CSL under tension



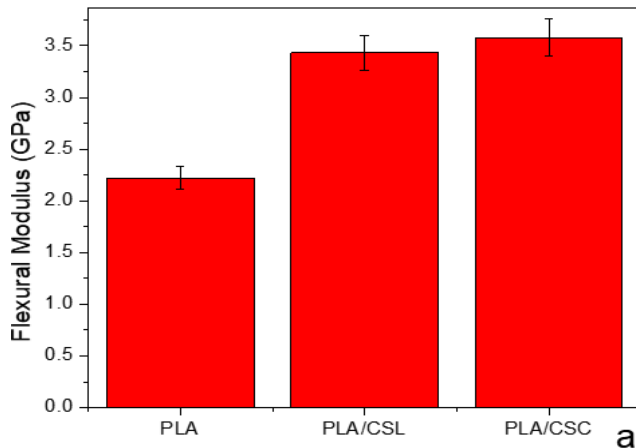


Figure 4: (a) Flexural modulus of PLA, PLA/CSC, and PLA/CSL

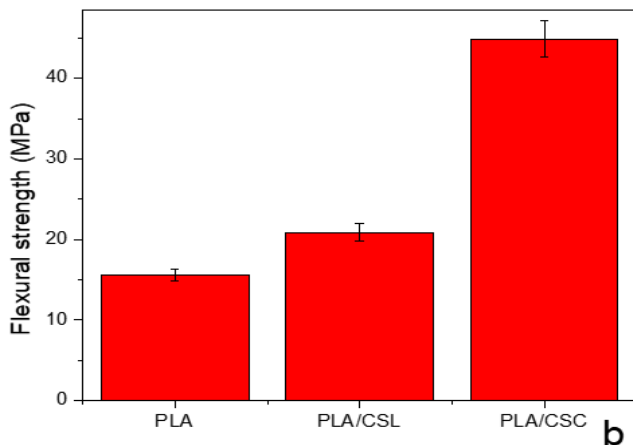


Figure 4: (b) Flexural strength of PLA, PLA/CSC, and PLA/CSL

Flexural strength and modulus of samples presented in Figure 3a-b indicate that using CSL and CSC improves these properties in PLA. The addition of 20 wt. % CSC to PLA heightens the flexural modulus and strength of PLA by 61.2 and 187.8 %, respectively. This composite (PLA/CSC) possesses the highest magnitude of both flexural modulus and strength. Cornstalk lignin also improves these properties in PLA, but their magnitudes are lower than PLA/CSC. The improved flexural properties of the composites suggest an indication of proper stress transfer at the matrix/reinforcement interphase [47]. Hydrogen bonds in cellulose have been reported to improve interfacial bonding energy that boosts the flexural strength of a composite [48]. This is also in line with the investigation of Zhang et al. [49], who synthesized lignin-polyamide 12 composite via 3D printing. The hydrogen bonding (generated from the OH and C₆H₅OH contents in lignin) improved the interaction between the matrix and reinforcement and

led to an increase in the composite’s flexural strength.

3.3 Morphological Study

Figure 5a-c shows the SEM morphologies (fractured surfaces after tension) of PLA, PLA/CSL, and PLA/CSC. A cracked surface with PLA flakes exists in the fracture micrograph of PLA (Figure 5a), while more cracks are revealed on the fractured surface of PLA/CSL composite (Figure 5b). The fractured surface appears rougher compared to that of PLA, and it possesses finer matrix flakes. Agglomeration of reinforcement is not evident in the morphology of the PLA/CSL fractured surface; this is also similar to that of PLA/CSC (Figure 5c), whose fractured surface is devoid of reinforcement agglomeration. Its surface is rougher than that of PLA/CSL, which justifies its best performance under tension (elastic modulus, yield, tensile, and fracture strengths) of the three polymer samples. Cellulose and lignin offer mechanical strengths to plants [50-51] as a result of their intrinsic stiffness engendered by extensive hydrogen bonding in their structures. The stiffness of these polysaccharides is responsible for the increase in tensile loads (when compared to that of PLA) required in deforming each composite to complete fracture. Pulling these samples apart, therefore, creates a rough surface in the composites. This also justifies the reason why the elongation at break follows the order: PLA/CSC>PLA/CSL>PLA.

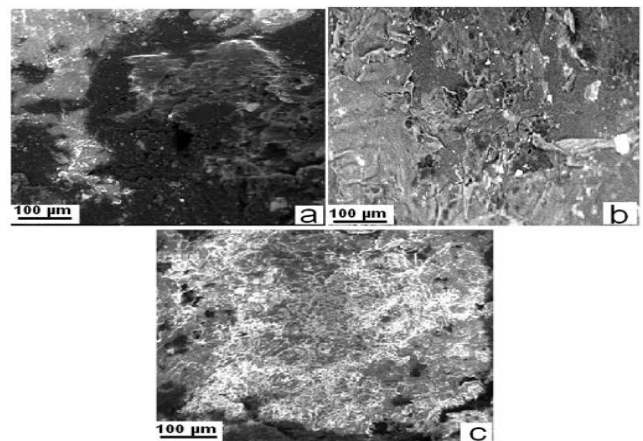


Figure 5: SEM of fractured surfaces after tensile tests (a) PLA (b) PLA, PLA/CSL (c) PLA/CSC

4.0 CONCLUSION

In this work, cellulose (CSC) and lignin (CSL) have been successfully synthesized from cornstalk (CS). The average E_H calculated from the combined intra and intermolecular hydrogen bonding interactions in CSC is calculated to be 4.63 kCal, while that from CSL is calculated to be 4.47 kCal. In addition to this,



the average R 2.78 Å is maintained by CSC, which is \approx 2.8 % lower than that of CSL. This implies that the shorter the magnitude of R , the stronger the bond strength. As reinforcement in PLA, the higher magnitude of average E_H in CSC is responsible for PLA/CSC displaying a UTS of 67 MPa, 54.8 MPa yield strength, 2.32 GPa elastic modulus, and 4.7 % elongation. Although both composites showed improved mechanical performances compared to unreinforced PLA, PLA/CSC showed a better response of the two. This study thus confirms that the hydrogen bonds in biomass cellulose and lignin play a major role in the mechanical performance of a polymer composite. Changing the mechanical properties of a polymer matrix can thus be influenced by altering the hydrogen bonds in CSC and CSL, which can be achieved by employing different polysaccharide isolating methods. Composites such as PLA/CSC and PLA/CSL developed in this study can be used as structural supporting devices in soft tissue engineering; reinforcing materials with the matrix are both biodegradable, and the mechanical properties fall within those possessed by soft tissues in humans. This work has only established the efficacy of CSC and CSL hydrogen bond interactions in PLA; further work will examine the influence of other extraction methods on their bond structure, composites' biodegradation (*In Vitro*), antimicrobial features, and glass-transition temperature.

REFERENCES

- [1] Karan, P. and Chakraborty, R. "Biopolymers for Tissue Engineering", *ACSSYMPOSIUM SERIES*, 1487, p. 259-276, 2024. Doi:10.1021/bk-2024-1487.ch011
- [2] Taghizadeh-hesary, F. Rasoulinezhad, E. Yoshino, N. Chang, Y. Taghizadeh-hesary, F. and Morgan, P. "The Energy–Pollution–Health Nexus: A Panel Data Analysis of Low-and Middle-Income Asian Countries," *The Singapore Economic Review*, 66(2), p. 435-455, 2021. <https://doi.org/10.1142/S0217590820430043>
- [3] Oladunni, O. J. Mpofo, K. and Olanrewaju, O.A. "Greenhouse Gas Emissions and its Driving Forces in the Transport Sector of South Africa", *Energy Reports*, 8, p. 2052-2061, 2022. <https://doi.org/10.1016/j.egy.2022.01.12>
- [4] Pires, J.B. Santos, F. N. Cruz, E. P. Fonseca, L.M. Pacheco, C.O. Rosa, B.N. Santana, L.R. Pereira, C.M.P. Carreno, N.L.V. Diaz, P.S. Zavareze, E.R. and Dias, A.R.G. "Cassava, Corn, Wheat, and Sweet Potato Native Starches: A Promising Biopolymer in the Production of Capsules by Electrospinning", *International Journal of Biological Macromolecules*, 281, p. 1-15, 2024. <https://doi.org/10.1016/j.ijbiomac.2024.136436>
- [5] Gbenebor, O. P. Adeosun, S. O. Adegbite, A.A. and Akinwande, C. "Organic and Mineral Acid Demineralizations: Effects on Crangon and Liocarcinus Vernalis–Sourced Biopolymer Yield and Properties", *Journal of Taibah University for Science*, 12(6), p. 837-845, 2018. <https://doi.org/10.1080/16583655.2018.1525845>
- [6] Odili, C. C. Ilomuanya, M. O. Sekunowo, O.I. Gbenebor, O.P. and Adeosun, S.O. "Knot Strength and Antimicrobial Evaluations of Partially Absorbable Suture", *Progress in Biomaterials*, 12, p. 51-59, 2023. <https://doi.org/10.1007/s40204-022-00212-8>
- [7] Nath, P. C. Sharma, R. Mahapatra, U. Mohanta, Y.K. Rustagi, S. Nayak, P.K. and Sridhar, K. "Sustainable Production of Cellulosic Biopolymers for Enhanced Smart Food Packaging: An up-to-date Review", *International Journal of Biological Macromolecules*, 273, p. 1-18, 2024. <https://doi.org/10.1016/j.ijbiomac.2024.133090>
- [8] Miao, B. H. Headrick, B. J. Li, Z. Spanu, L. Loftus, D. J. and Lepech, M. D. "Development of Biopolymer Composites using Lignin: A Sustainable Technology for Fostering a Green Transition in the Construction Sector", *Cleaner Materials*, 14, p. 1-11, 2024. <https://doi.org/10.1016/j.clema.2024.100279>
- [9] Pande, D. C. Vu, T. H. Lu, Y. Sainsbury, F. Dau, V. T. and Rehm, H. A. "Restructuring Biologically Assembled Binding Protein-Biopolymer Conjugates Toward Advanced Materials", *ACS Applied Materials & Interfaces*, 16, p. 68983-68995, 2024. <https://pubs.acs.org/doi/10.1021/acsami.4c15941>
- [10] Ochulor, E. F. Gbenebor, O. P. and Lawal, I. O. "Physicochemical, Morphology and Functional Group Analyses of Gelatin Extracted from Croaker Fish (*Pseudotolithus senegalensis*) Dcale for Suitability in Biomedical Applications", *Nigerian Research Journal of Engineering and Environmental Sciences*, 7(2), p. 436-446, 2022.
- [11] Fatchurrohman, N. Muhida, K. and Maidawat. "From Corn to Cassava: Unveiling PLA Origins for Sustainable PLA 3D Printing",



- Journal Teknologi*, 13(3), p. 87-93, 2023.
<https://doi.org/10.35134/jitekin.v13i2.101>
- [12] Pinos, J. A. "Thermo-mechanical Study of the Mixture of Polylactic Acid PLA Obtained from Potato Starch with an Aliphatic Copolyester PBSA (polybutylene Succinate Adipate)", *Revista DYNA*, 89(221), p. 142-150, 2022.
<https://doi.org/10.15446/dyna.v89n221.98414>
- [13] Scaffaro, R. Maio, A. Gulino, E. F. and Micale, G.D.M. "PLA-Based Functionally Graded Laminates for Tunable Controlled Release of Carvacrol Obtained by Combining Electrospinning with Solvent Casting", *Reactive and Functional Polymers*, 148, p. 1-9, 2020.
<https://doi.org/10.1016/j.reactfunctpolym.2020.104490>
- [14] Vălean, C. Linul, E. Palomba, G. and Epasto, G. "Single and Repeated Impact Behavior of Material Extrusion-Based Additive Manufactured PLA Parts", *Journal of Materials Research and Technology*, 30, p. 1470-1481, 2024.
<https://doi.org/10.1016/j.jmrt.2024.03.150>
- [15] Alex, Y. Divakaran, N. C. Pattanayak, I. Lakshyajit, B. Ajay, P. V. and Mohanty, S. "Comprehensive Study of PLA Material Extrusion 3D Printing Optimization and its Comparison with PLA Injection Molding through life Cycle Assessment", *Sustainable Materials and Technologies*, 43, p.1-17, 2025.
<https://doi.org/10.1016/j.susmat.2024.e01222>
- [16] Akpan, E. I. Gbenedor, O. P. Igogori, E. A. Aworinde, A. K. Adeosun, S. O and Olaleye, S. A. "Electrospun Bio-Fibre Mat Based on Polylactide / Matural Fibre Particles", *Arab Journal of Basic and Applied Sciences*, 26(1), p. 225-235, 2019.
<https://doi.org/10.1080/25765299.2019.1607995>
- [17] Eraslan, A. Altinbay, and Nofar, M. "In-situ Self-Reinforcement of Amorphous Polylactide (PLA) through Induced Crystallites Network and its Highly Ductile and Toughened PLA/poly (butylene Adipate-co-Terephthalate) (PBAT) Blends", *International Journal of Biological Macromolecules*, 272, p. 1-12, 2024.
<https://doi.org/10.1016/j.ijbiomac.2024.132936>
- [18] Wang, W. Niu, B. Liu, R. Chen, H. Fang, X. Wu, W. Wang, G. Gao, H. and Mu, H. "Development of Bio-Based PLA/Cellulose Antibacterial Packaging and its Application for the Storage of Shiitake Mushroom", *Food Chemistry*, 429, p. 1-12, 2023.
<https://doi.org/10.1016/j.foodchem.2023.136905>
- [19] Gbenedor, O. P. Ochulor, E. F. Shogunwa, A. A. and Adeosun, S. O. "Evaluation Studies of Hydrogen Bond, Crystallinity and Water Propensity of Treated Bambusa Vulgaris Cellulose Particles", *Nigerian Research Journal of Engineering and Environmental Sciences*, 7(1), p. 260-272, 2022.
10.5281/zenodo.6725623
- [20] Zhang, Z. Wang, W. Li, Y. Fu, K. Tong, X. Cao, B. and Chen, B. "3D Printing of Cellulose Nanofiber/Polylactic Acid Composites via an Efficient Dispersion Method", *Composites Communications*, 43, p. 1-5, 2023.
<https://doi.org/10.1016/j.coco.2023.101731>
- [21] Agbakoba, V. C. Mokhena, T. C. Ferg, E. E. Hlangothi, S. P. and John, M. J. "PLA Bio-Nanocomposites Reinforced with Cellulose Nanofibrils (CNFs) for 3D Printing Application", *Cellulose*, 30, p. 11537–11559, 2023.
<https://link.springer.com/article/10.1007/s10570-023-05549-2>
- [22] Bononad, P. C. Freitas, P. A. V. Martínez, C. G. Chiralt, A. and Vargas, M. "Influence of the Purification Degree of Cellulose from *Posidonia oceanica* on the Properties of Cellulose-PLA Composites", *Polysaccharides*, 5, p. 807-822, 2024.
<https://doi.org/10.3390/polysaccharides5040050>
- [23] Gbenedor, O. P. Odili, C. C. Obasa, V. D. Ochulor, E. F. Kusoro, S. O. Udogu-Obia, O. C. and Adeosun, S. O. "Morphological, Mechanical and Thermal Characteristics of PLA /Cocos nucifera L Husk and PLA/Zea mays Chaff Lignin Fibre Mats Composites", *Nigerian Journal of Technological Development*, 20(4), p. 1-9, 2023.
10.4314/njtd.v20i4.1561
- [24] Shar, A. S. Wang, N. Chen, T. Zhao, X. Weng, Y. "Development of PLA/Lignin Bio-Composites Compatibilized by Ethylene Glycol Diglycidyl Ether and Poly (ethylene glycol) Diglycidyl Ether", *Polymers*, 15, p. 1-11, 2023.
<https://doi.org/10.3390/polym15204049>
- [25] Ren, Z. Zhou, X. Ding, K. Ji, T. Sun, H. Chi, X. Wei, Y. Xu, M. Cai, L. and Xia, C. "Design of Sustainable 3D Printable Polylactic Acid Composites with High Lignin Content", *International Journal of Biological*



- Macromolecules*, 253, p. 1-11, 2023. <https://doi.org/10.1016/j.ijbiomac.2023.127264>
- [26] Ou, W. X. Weng, Y. Zeng, J. and Li, Y. D. “Fully Biobased Poly (lactic Acid)/Lignin Composites Compatibilized by Epoxidized Natural Rubber”, *International Journal of Biological Macromolecules*, 236, p. 1-9, 2023. <https://doi.org/10.1016/j.ijbiomac.2023.123960>
- [27] Ye, H. He, Y. Li, H. You, T. and Xu, F. “Customized Compatibilizer to Improve the Mechanical Properties of Polylactic Acid/Lignin Composites via Enhanced Intermolecular Interactions for 3D Printing”, *Industrial Crops and Products*, 206, p. 1-11, 2023. <https://doi.org/10.1016/j.indcrop.2023.117454>
- [28] Zaidi, S. A. S. Kwan, C. E. Mohan, D. Harun, S. Luthf, A.A.I. and Sajab, M.S. “Evaluating the Stability of PLA-Lignin Filament Produced by Bench-Top Extruder for Sustainable 3D Printing”, *Materials*, 16, p. 1-12, 2023. <https://doi.org/10.3390/ma16051793>
- [29] Igathinathane, C. Womac, A. C. and Sokhansanj, S. “Corn Stalk Orientation Effect on Mechanical Cutting”, *Biosystems Engineering*, 107, p. 97-106, 2010. <https://doi.org/10.1016/j.biosystemseng.2010.07.005>
- [30] Zeng, K. He, X. Yang, H. Wang, X. and Chen, H. “The Effect of Combined Pretreatments on the Pyrolysis of Corn Stalk”, *Bioresource Technology*, 281, p. 309-317, 2019. <https://doi.org/10.1016/j.biortech.2019.02.107>
- [31] Gbenebor, O. P. Osabumwenre, F. O. and Adeosun, S. O. “Structural, Mechanical and Thermal Properties of Low-Density Polyethylene/Biomass Composite: Effects of Particle Size”, *Kufa Journal of Engineering*, 11(2), p. 67-83, 2020.
- [32] Gbenebor, O. P. Olanrewaju, O. A. Usman, M.A. and Adeosun, S.O. “Lignin from Brewers’ Spent Grain: Structural and Thermal Evaluations”, *Polymers*, 15(10), p.1-14, 2023. <https://doi.org/10.3390/polym15102346>
- [33] Rasheed, H. A. Adeleke, A. A. Nzerem, P. Olosho, A. I. Ogedengbe, T. S. and Jesuloluwa, S. “Isolation, Characterization and Response Surface Method Optimization of Cellulose from Hybridized Agricultural Wastes”, *Scientific Reports*, p. 1-15, 2024. <https://doi.org/10.1038/s41598-024-65229-4>
- [34] Srinivasan, S. and Venkatachalam, S. “One Pot Green Process for Facile Fractionation of Sorghum Biomass to Lignin, Cellulose and Hemicellulose Nanoparticles using Deep Eutectic Solvent”, *International Journal of Biological Macromolecules*, 277, p. 1-15, 2024. <https://doi.org/10.1016/j.ijbiomac.2024.134295>
- [35] Ciolacu, D. Kovac, J. and Kokol, V. “The effect of the Cellulose-Binding Domain from Clostridium Cellulovorans on the Supramolecular Structure of Cellulose Fibres”, *Carbohydrate Research*, 345, p. 621-630, 2010. <https://doi.org/10.1016/j.carres.2009.12.023>
- [36] Gbenebor, O. P. Adeosun, S. O. Lawal, G. I. and Jun, S. “Role of CaCO₃ in the Physicochemical Properties of Crustacean-Sourced Structural Polysaccharides”, *Materials Chemistry and Physics*, 184, p. 203-209, 2016. <https://doi.org/10.1016/j.matchemphys.2016.09.043>
- [37] Gbenebor, O. P. Adeosun, S. O. Lawal, G. I. Jun, S. and Olaleye, S.A. “Acetylation, Crystalline and Morphological Properties of Structural Polysaccharide from Shrimp Exoskeleton”, *Engineering Science and Technology, an International Journal*, 20, p. 1155–1165, 2017. <https://doi.org/10.1016/j.jestch.2017.05.002>
- [38] Kubo, S. and Kadila, J. F. “Hydrogen Bonding in Lignin: A Fourier Transform Infrared Model Compound Study”, *Biomacromolecules*, 6, p. 2815-2821, 2005.
- [39] Poletto, M. and Zattera, A. J. “Materials Produced from Plant Biomass. Part III: Degradation Kinetics and Hydrogen Bonding in Lignin”, *Materials. Research*, 16(5), p. 1065-1070, 2013. <https://doi.org/10.1590/S1516-14392013005000112>
- [40] Pimentel, G. C. and Sederholm, C. H. “Correlation of Infrared Stretching Frequencies and Hydrogen Bond Distances in Crystals”, *The Journal of Chemical Physics*, 24, p. 639-641, 1955. 10.1063/1.1742588
- [41] Hasheminejad, K. and Montazeri, A. “Enhanced Interfacial Characteristics in PLA/Graphene Composites Through Numerically-Designed Interface Treatment”, *Applied Surface Science*, 502, p. 1-11, 2020. <https://doi.org/10.1016/j.apsusc.2019.144150>
- [42] Xia, Y. Li, X. Zhuang, J. Wang, W. Abbas, S. C. Fu, C. Zhang, H. Chen, T. Yuan, Y. Zhao, X. and Ni, Y. “Exploitation of Function Groups in Cellulose Materials for Lithium-Ion



- Batteries Applications”, *Carbohydrate Polymers*, 325, p. 1-29, 2024. <https://doi.org/10.1016/j.carbpol.2023.121570>
- [43] Zhao, J. Zhang, Y. Cong, H. Zhang, C. and Wu, J. “Quantifying the Contribution of Lignin to Humic Acid Structures During Composting”, *Chemical Engineering Journal*, 492, p. 1-10, 2024. <https://doi.org/10.1016/j.cej.2024.152204>
- [44] Gorgun, E. Ali, A. and Islam, M. S. “Biocomposites of Poly (Lactic Acid) and Microcrystalline Cellulose: Influence of the Coupling Agent on Thermomechanical and Absorption Characteristics”, *ACS OMEGA*, 9, p. 11523–11533, 2024.
- [45] Johansson, M. Skrifvars, M. Kadi, N. and Dhakal, H. “Effect of Lignin Acetylation on the Mechanical Properties of Lignin-Polylactic Acid Biocomposites for Advanced Applications”, *Industrial Crops and Products*, 202, p. 1-11, 2023. [10.1016/j.indcrop.2023.117049](https://doi.org/10.1016/j.indcrop.2023.117049)
- [46] Makri, S. Xanthopoulou, E. Klonos, P. A. Grigoropoulos, A. Kyritsis, A. Tsachouridis, K. Anastasiou, A. Deligkiozi, I. Nikolaidis, N. and Bikiaris, D. N. “Effect of Micro- and Nano-Lignin on the Thermal, Mechanical, and Antioxidant Properties of Biobased PLA–Lignin Composite Films”, *Polymers*, 14, p. 1-25, 2022. <https://www.mdpi.com/2073-4360/14/23/5274>
- [47] Ruz-Cruz, M. A. Franco, P. J. F. Johnson, E.A.H. Chulim, M.V.M. Manzano, L.M.G. and González, A.V. “Thermal and Mechanical Properties of PLA-Based Multiscale Cellulosic Biocomposites”, *Journal of Materials Research and Technology*, 18, p. 485-495, 2024. <https://doi.org/10.1016/j.jmrt.2022.02.072>
- [48] Ben, Y. Luo, H. Liu, W. Ba, Z. Cui, J. Guo, Z. and Sun, R. “Robust Flexural Performance of Modified Bamboo through Strategic Delignification and Carboxymethyl Cellulose Modification”, *Composites Part A: Applied Science and Manufacturing*, 190, p. 1-31, 2025. <https://doi.org/10.1016/j.compositesa.2024.108655>
- [49] Zhang, S. Ji, A. Meng, X. Bhagia, S. Yoo, C.G. Harper, D.P. Zhao, X. Ragauskas, A.J. “Structure-Property Relationship between Lignin Structures and Properties of 3D-Printed Lignin Composites”, *Composites Science and Technology*, 249, p. 1-10, 2024. <https://doi.org/10.1016/j.compscitech.2024.110487>
- [50] Schuetz, M. Benske, A. Smith, R. A. Watanabe, Y. Tobimatsu, Y. Ralph, J. Demura, T. Ellis, B. and Samuels, A.L. “Laccases Direct Lignification in the Discrete Secondary Cell Wall Domains of Protoxylem”, *Plant Physiology*, 66, p. 798–807, 2014. <https://doi.org/10.1104/pp.114.245597>
- [51] Riseh, R.S. “Advancing Agriculture through Bioresource Technology: The Role of Cellulose-Based Biodegradable Mulches”, *International Journal of Biological Macromolecules*, 255, p. 1-10, 2024. <https://doi.org/10.1016/j.ijbiomac.2023.128006>

